pH-Responsive Nanoparticles for Controlled Release

José Gonçalves

CQE and IN, Instituto Superior Técnico, Universidade de Lisboa, Portugal

Abstract Among a variety of inorganic-based nanomaterials, mesoporous silica particles (MSNs) have several attractive features for application as a drug delivery system due to their high surface areas, large pore volumes, uniform and tunable pore sizes, and a great diversity of surface functionalization options. A novel pH-responsive Drug Delivery System (DDS), composed of a mesoporous silica nanostructure coated with a pH-responsive polymeric shell was synthesized. The particles were modified with amine groups using APTES, which were used to immobilize Chain Transfer Agent (CTA) molecules for the controlled polymerization of 2-(diisopropylamino)ethyl methacrylate (DPA) from the surface. The polymer-coated MSNs were obtained using a hybrid grafting approach. The hybrid nanoparticles have diameters around 56 nm at pH values lower than 6.5. Our proof-of-concept system shows that by modulating the pH, it is possible to achieve a pumping regime that modifices the release rate in a controlled way.

Key-Words: hybrid nanoparticles, mesoporous silica nanoparticles, RAFT, pH-response, polymeric shell, controlled release

1. Introduction

During the last decades of the 20th century, a substantial effort was made to move from sustained, but essentially uncontrolled, release systems (e.g., waxes and other polymeric matrices) to controlled-release systems such as transdermal patches and improved oral-inhalation formulations. In the 1990s, the appearance of new drugs with larger molecular sizes, higher dose sensitivities, and often poorer stabilities in biological environments led to a stronger push towards the development of efficient encapsulation and controlled-release technologies. [1]

From a technological perspective, controlled drug delivery implies the ability to control the distribution of therapeutic agents both in space and time. [2] Successful targeting, requires the production of the DDSs in the form of nanoparticles (NPs) that can breach biological barriers to reach their specific target. To cater for the various delivery options, a wide range of particulate-delivery systems (organic and inorganic) has been designed. [3]

The blood stability represents a major problem for all delivery systems. In the blood, protein markers (opsonins) adsorb on the surface of hydrophobic carriers, thus providing a signal to the immune system to evacuate these foreign entities from the body. Thus, to enhance circulation time, the surface of the carrier needs to be functionalized with hydrophilic molecules in order to avoid detection by the immune system. This additional requirement disturbs the production process significantly [4]

The hydrodynamic stability in the blood stream is achieved by keeping the particle size between 50 and 300 nm. [1]

Mesoporous silica nanoparticles (MSNs) have attracted substantial attention due to their versatile structural properties, such as high specific surface area and large pore volume, colloidal stability, and the possibility to specifically functionalize the inner pore system and/or the external particle surface. These properties provide unique advantages to encapsulate a variety of therapeutic agents and deliver these agents to the desired location. Additionaly, the size, morphology, pore size, and pore strucuture of MSNs can be rationally designed accordingly to the desired application, using surfactants as structure-directing agents (SDAs). [5]

In 1968, Stöber first discovered an effective method for the synthesis of monodispersed silica particles, which involves the hydrolysis of tetralkyl silicates in a mixture of alcohol and water using ammonia as a catalyst. [6] With a careful choice of the template and control of the self-assembly and silica condensation rate, it is possible to tailor the sizes, mesostructures and morphologies of the mesoporous silica nanoparticles. [7]

The series of mesoporous materials, named Mobil Composition of Matter (MCM), first synthesized in 1992 by Mobil's researchers, have been keenly studied by researchers. MCM-41 and MCM-48 have attracted the most attention, due to their striking property of possessing a long range ordered framework with ordered mesopores, albeit being composed by amorphous silica wall. [8] However, the material obtained, yields particles with 1 µm or higher in size, with a wide size distribution. It was reported that by modifying the Stöber synthetic compositions and by adding a cationic surfactant to the reaction

mixture, spherical silica particles featuring an MCM-41 structure were obtained, instead of the hexagonal prisms. [9]

Hybrid nanoparticles composed of an inorganic core and a polymer shell have attracted great interest due to the intriguing properties associated with the nanocomposites. [10] It is generally accepted that nanoparticles with neutral and hydrophilic surface will have a longer blood circulation half-life. As such, the coating of the nanoparticles with a hydrophilic polymer (e.g. stealth coating) is the most commonly used method to modify the nanoparticle surface properties. However, nanoparticles composed by silica-polymer core-shell are hard to obtain, due to the incompatibility between inorganic-organic materials. Therefore, the synthesis of these NPs is assisted by functionalization of silica surface, leading to an increased compatibility between the two phases. [11]

The current large interest in responsive polymers has arisen due to their ability to undergo reversible conformational changes in solution (solubility, conformation in solvent, etc) as a function of the external environment. For drug release, pH and temperature are the most important stimuli. Temperature is called an external stimulus since it must be changed by a source external to the organism. pH, on the other hand, is called an internal stimulus since changes within the body. Therefore, it can be used to direct the response to a certain tissue or cellular compartment without any external help. [12] Furthermore, there are subtle changes within different tissues that make pH-responsive delivery an effective strategy. [13]

Reversible addition-fragmentation chain transfer (RAFT) has emerged as promising CRP technique due to its versatility and simplicity, and the polymer is free from the contamination of metal catalyst. The mechanism of addition-fragmentation is based on the reaction between a propagating radical and a chain transfer agent, which bears both an activated double bond and a weak bond. Addition of the propagating radical to the unsaturation induces the formation of an intermediate radical which undergoes a fragmentation reaction that involves the weak bond. The released radical enters the polymerization cycle. [14]

In reversible deactivation radical polymerization (RDRP), such as RAFT polymerization, the ideal conditions can be mimicked in the presence of chain transfer agents (CTAs), that induce reversible addition-fragmentation transfer reactions. The RAFT agent controls and directs the polymerization, allowing the chains to grow at the same rate. [15]

The aim of this work was to develop hybrid mesoporous silica nanoparticles with silica nanostructured core and a shell of pH-responsive polymer. The biocompatible polymer used is based on a polybase of a tertiary amine methacrylate, 2-(diisopropylamino)ethyl methacrylate (DPA). This hybrid system is a good candidate as drug delivery system with interesting applications on cancer treatment. This type of systems can take advantage of the polymeric conformational transition since its occurs in the pH range of tumour cells. The mechanism expected for controlled drug release is illustrated in Scheme 1. In a basic/neutral medium (pH > 6.5), the polymeric shell exhibits hydrophobic behaviour due to its deprotonation, allowing a collapsed (unswollen) conformation that protects the drug loaded inside the MSN pores from diffusion. On the other hand, when the medium becomes acidic (pH < 6.5), the polymer protonates turning into a cationic soluble polyelectrolyte due to the protonation of its amine, showing an extended (swollen) conformation, that allows a gradual diffusion of the drug molecule into the medium.

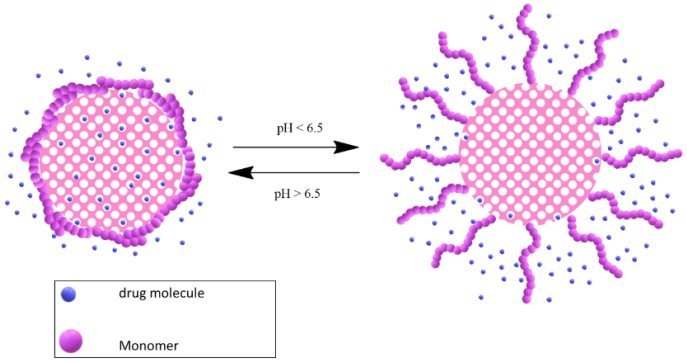

Scheme 1 - Schematic ilustration of the expected controlled release mechanism by MSN+PolyDPA.

2. Experimental

2.1 Materials

Absolute Ethanol (99.9 % EtOH, Scharlau), hexadecyltrimethylammonium bromide (99 % CTAB, Sigma-Aldrich), sodium hydroxide (Pure NaOH, EKA Pellets, Bohus, Sweden) and tetraethoxysilane (99 % TEOS, Sigma-Aldrich) were all used as received for synthesis of mesoporous silica nanoparticles (MSNs). The dye incorporated into MSNs, PDI derivative, was synthesized according to the literature. [16] (3-Aminopropyl) triethoxysilane (98 % APTES, Sigma-Aldrich), without any treatment, was used for surface modification in dry toluene which was distilled over calcium hydride before use. The surfactant templates were removed

using a 0.5 M hydrochloric acid solution (37 % HCl, AnalaR NORMAPUR – VWR) in absolute EtOH. For chain transfer agent (CTA) immobilization, N-(3-dimethylaminopropyl) -N′-ethylcarbodiimide (98 % EDC, Sigma-Aldrich) in dry dichloromethane and 3-(benzylsulfanylthiocarbonylsulfanyl) propionic acid (BSPA) or 4-Cyano-4-(phenylcarbonothioylthio)pentanoic acid (CPADB, 97 %, Sigma-Aldrich) as CTA, were used. In order to synthesize the monomer 2–(diisopropylamino) ethyl methacrylate (DPA), hydroquinone (99 %, Aldrich Chemistry), methacryloyl chloride (97 %, Aldrich), and 2–(diisopropylamino) ethanol (98 %, Aldrich Chemistry) were all used as received. Also, tetrahydrofuran (99 % THF, Aldrich) dried with sodium and dry triethylamine distilled over calcium hydride were used. For the RAFT polymerization of 2–(diisopropylamino) ethyl methacrylate, tetrahydrofuran (99.9 % THF, Aldrich), azobisisobutyronitrile (AIBN, 99 %, Sigma-Aldrich) recrystallized, Trifluoroacetic acid (>99 %, Merck), absolute EtOH and 1,4 - Dioxane previously dried with sodium and distilled were used. Sodium dihydrogen phosphate monohydrate (NaH_2PO_4, 98%, Panreac), disodium hydrogen phosphate (Na_2HPO_4, 99%, Riedel-de-Haen) and sodium hydroxide (NaOH, 98%, Sigma-Aldrich) were used to prepare the phosphate buffer solutions (PBS, 100 mM pH 5 and pH 9). Sulforhodamine B (SRB, Molecular Probes) was used as a model molecule for the release studies. Deionized water from a Millipore system Milli-Q ≥18 MΩ cm (with a Millipak membrane filter 0.22 µm) was used in the preparation of solutions and in synthesis.

2.2. MSNs synthesis

MSNs were synthesized by a modified sol-gel process. In a 15 mL polypropylene flask, CTAB (0.5 g) and PDI (1.6 mg) were mixed in THF (5 mL). The mixture was sonicated in order to dissolve the PDI and was left stirring at 40 ℃ until THF was evaporated (approximately 24 h). In a 500 mL polypropylene flask, deionized (DI) water (240 mL) and a NaOH solution (1 M or 1.7 M, 1.75 mL) were added. After the temperature inside the flask was stabilized at 32 ℃, the solid mixture CTAB/PDI was added. After 30 min, TEOS (2.5 mL) was added dropwise, and the solution was left stirring for 3 h. The MSNs were recovered by centrifugation at 30,000 × g for 20 min at 20 ℃ and washed twice with a mixture of ethanol and water (50% v/v) and once with absolute ethanol, discarding each time the supernatant. Alternatively, MSNs were recovered by filtration under vacuum. The solid product obtained was dried at 323.15 K overnight. Finally, the particles were dried under vacuum.

2.3. Modification of MSNs Surface

Amino modification of the silica was performed by suspending the obtained nanoparticles in dry toluene (18 mL per 500 mg of nanoparticles) and sonicating it for 15 min, under argon atmosphere. Afterwards, APTES (0.15 mL) was added dropwise and the resulting mixture was put under reflux (T= 130 ℃) for 24h under argon atmosphere. The solid product (MSN+APTES+CTAB) was obtained by centrifugation at 13081 rpm for 10 min at 18 ℃., and washed three times with absolute ethanol, discarding each time the supernatant. The particles were dried in a ventilated oven for 24 h at 323.15 K. An acidic ethanol solution ([HCl] = 0.5 M, 25 mL per 500 mg of MSN) was used to remove the template, by re-suspending MSN+APTES+CTAB and sonicating it for 15 min. Subsequently, it was left under stirring at 50 ℃ for 24 h. MSN+APTES were recovered by centrifugation at 13081 rpm for 10 min at 18 ℃ and washed once with a basic ethanol solution (NH_4 25%v/v) and five times with absolute ethanol, until until neutralization of the supernatant. The product was dried at 50 ℃ under vacuum for 24h.

In order to immobilize CTA on the nanoparticles' surface 15 mL of dry dichloromethane was added per 250 mg of MSN+APTES into a 25 mL flask under argon atmosphere and sonicated for 20 minutes. Then, 3-(benzylsulfanylthiocarbonylsulfanyl) propionic acid (BSPA) or 4-Cyano-4-(phenylcarbonothioylthio)pentanoic acid (CPADB) (1 eq to APTES) was added to the mixture, at low temperature. After 10 min, EDC (1.2 eq to APTES) was added and the mixture was left stirring, under argon atmosphere, at room temperature for 24h. MSN+CTA were recovered by centrifugation at 12000 rpm for 10 min at 18 ℃., and washed three times with absolute ethanol, discarding each time the supernatant.

2.4. Kinetics of RAFT Polymerization

Route 1 In a Schlenk tube 8.2 mg of BSPA were added under vacuum. Afterwards, under argon atmosphere, 1,4-dioxane (0.5 mL), DPA (0.33 mL, 1 eq) and a solution of AIBN in 1,4-dioxane ([AIBN] = 1mg/mL, 0.5 mL)) were added. The molar ratio of AIBN and CTA was kept constant (1:10). Atmosphere oxygen was removed by bubbling the solution with argon for 1 h. Finally, the mixture was put in a bath at the desired temperature (70 ℃, 80 ℃ or 90 ℃) for 24h. Samples were taken in intervals of 15 min

during the first hour, and 30 min for the next 3 h. The polymer was precipitated with diethyl ether and the Schlenk was washed to remove residues. Then, the polymer was dissolved in methanol and evaporated until dryness. Finally, it was put under vacuum and a foam was formed.

Route 2 500 mg of DPA (1 Eq.), 220 µL of TFA and 0.5 mL of absolute EtOH were stirred in a vial for 10min. After, 1.7 mg of AIBN and 14.4 mg of CPADB were added separately with EtOH (1:5 AIBN/RAFT). The AIBN solution was first transferred to the vial with CTA, and the resulting mixture transferred to the vial containing the monomer. In each transfer the vials were washed with EtOH. Finally, the mixture was transferred to a Schlenk tube and left under argon atmosphere. The total volume of EtOH was 1.8 mL. The oxygen was removed with five freeze-pump cycles. The mixture was then placed in an oil bath at 80 ℃ for 5h. The polymer was precipitated with diethyl ether and the Schlenk was washed to remove residues. Then, the polymer was dissolved in ethanol and evaporated until dryness. Finally, it was dried under vacuum and a solid product was formed.

2.5. Polymer grafting to the MSN surface

A Schlenk tube (A) was prepared containing 100 mg of MSN4+CPADB and 0.27 mg of AIBN (molar ratio AIBN/RAFT: 1:5) under argon atmosphere. In a separate Schlenk tube (B) a polymerization reaction was conducted as described for the kinetic study, using two times the quantity of CTA present in the Schlenk A. At 3h (≈50% conversion, see section 3.5.), the mixture from B was transferred to Schlenk A with a cannula under argon and left at 80 ℃ for 24h. The particles were recovered by centrifugation at 12000 rpm for 10 min at 18 ℃., and washed three times with absolute ethanol, keeping each supernatant. The solid product obtained was dried at 50 ℃ overnight. Finally, the particles were dried under vacuum. The polymer present in the supernatant was precipitated with diethyl ether. After, the polymer was dissolved in ethanol and dry under vacuum and a solid product was formed.

2.6. Loading and Release of SRB

For loading and release of SRB, a ethanolic solution of SRB (3.90×10^{-3} M, 500 µL) was added to 1.5 mg of MSN+PolyDPA, and the dispersion was stirred overnight at room temperature. The dispersion was centrifuged (15000 rpm, 10 min at 20 ℃) to remove the unloaded SRB. The SRB loaded nanoparticles were redispersed in 1 mL of phosphate buffer (pH 9) and centrifuged. This procedure was repeated one more time, recovering the supernatants. In order to determine the molar absorption coefficient (ε) of SRB, several solutions were prepared in PBS at pH 9 and their absorption spectra were determined. Then, it was possible to determine the concentration of SRB in the supernatants obtained after the loading process

After the last centrifugation, the supernatant was removed and 200 µL of PBS (pH 9) was added to the loaded nanoparticles. The mixture was transferred to the dialysis device (Scheme 2, compartment A) and inserted on top of the fluorescence cuvette (previously filled with 3.2 mL of PBS (pH 9)), immediately before the beginning of the experiment. [17] SRB released from the nanoparticles was monitored through the fluorescence intensity of SRB ($\lambda_{excitation} = 566\,nm; \lambda_{emission} = 589\,nm$) on the bottom compartment (Scheme 2, compartment B) of the fluorescence cuvette, while modulating the pH between 5 and 9, with additions of H_2SO_4 (1 M, 10 µL) (300 s, 6000 s, 6540 s, 9020 s, 10600 s and 16500 s) and NaOH (1 M, 1 µL) (7880 s and 17700 s) for nearly 6 h. The additions were bottom in the dialysis device.

Scheme 2 - Schematic image of the dialysis device used in the release study. The dialysis tube with a cellulose membrane (A) contains 200 µL of PBS pH 9 and 1.5 mg of MSN+PolyDPA with SRB and the fluorescence cell (B) contains PBS pH 9.

The TEM apparatus used to characterize the MSN1, MSN2 and MSN3 was Hitachi transmission electron microscope of model H-8100 with LaB6 filaments (Hitachi, Tokyo, Japan). The accelerator voltage is 200 kV and the current is 20 µA. The images were acquired by the camera KeenView of Soft Imaging System, using the software iTEM. The SEM apparatus used to characterize the MSN4 was JEOL SEM (model JSM7001F, JEOL, Tokyo, Japan), with an accelerating voltage of 15 kV. The SEM samples were coated with chromium using a turbo-pumped sputter coater from Quorum Technology (model Q150T ES, Quorum Technology, Ashford, UK) for 1 min. Proton Nuclear Magnetic Resonance (^{1}H NMR) (δH) spectra were recorded on an AMX-400 instrument (Bruker, MA, USA). UV-660 UV-VIS Spectrophotometer (JASCO International, Tokyo, Japan), supplied with a double monochromator and a photomultiplier detector

for higher resolution, was employed for UV-Vis spectroscopy assays. Polymer shells were characterized by GPC-MALS in THF using a Waters 510 pump fitted with three columns (Phenolgel™ from Phenomenex, Torrance, CA, USA, with pore size 100, 1,000, and 10,000 Å; column temperature: 296.15 K) connected in series and a miniDAWN-treos multiangle laser light scattering detector from Wyatt Technologies (Santa Barbara, CA, USA) and a Waters 2410 refractive index detector at 303.15 K. Fluorescence measurements were obtained on a Horiba-JobinYvon Fluorolog-3 spectrofluorimeter using a fluorescent cell. Right angle geometry was used in all measurements.

3. Results

A novel pH-responsive Control-Release DDS, composed of a silica nanostructure core coated with a pH-responsive polymeric shell, was synthesized (Scheme 3).

3.1 MSNs Synthesis and characterization

A fluorescent dye was adsorbed to the structure of the surfactant hexadecyltrimethylammonium bromide (CTAB) (Step 1, Scheme 3). The MSNs were synthesized by the hydrolysis and condensation of tetraethoxysilane (TEOS) around the polar region of the CTAB micelles forming a silica structure around the surface of the micelles (Step 2, Scheme 3). To infer the impact of the pH in MSNs' size, solutions of different [NaOH] were used while maintaining the remain conditions (temperature, stirring, reactants and molar ratios).

MSNs size distribution was analyzed by TEM, SEM and DLS (20 ℃) (Figure 1) in order to estimate their diameters. (Table 1)

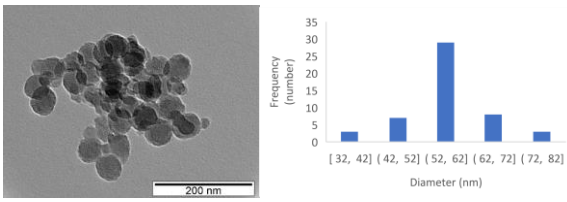

Figure 1 - TEM image (200 nm scale) obtained for MSN1 (left) and its histogram size distribution (right).

Table 1 - Particles' size obtain by TEM and DLS and respective standard deviation.

Sample	[NaOH] (M)	D_{TEM} (nm)	D_H (nm)
MSN1	1.7	56 ± 8	198 ± 72
MSN2	1.0	37 ± 3	75 ± 40
MSN3	1.7	57 ± 6	191 ± 21
MSN4	1.7	57 ± 9	182 ± 70

The diameters obtained from DLS are higher than the ones obtained from TEM as expected, since a hydrated layer is formed around MSN when the particles are dispersed.Even though, the values obtained from the two methods are different, both indicate that particles synthesized in the same conditions have identical sizes. MSNs synthesized in higher pH conditions are, as expected, larger than those produced in lower pH conditions. [18]

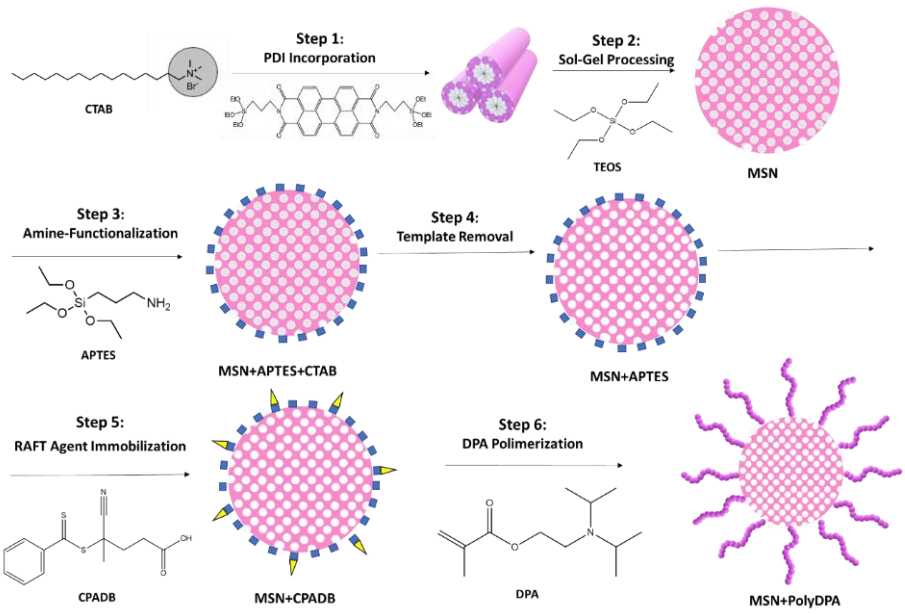

Scheme 3 - Schematic illustration for hybrid mesoporous silica nanoparticles prepared during this work.

3.2. Hybrid Nanoparticles

3.2.1. Amine Surface Modification of MSNs

After MSN synthesis, an amino surface modification was performed by adding (3-aminopropyl) triethoxysilane (APTES) to the silanol groups of the nanoparticles' external surface (Step 3, Scheme 3). The peak from the alpha-carbon to the silicon atom (less affected by possible interactions of the functional group) was used to estimate the number of organic molecules grafted onto the surface of MSNs, by comparing their integrated intensities with that of the internal standard. [19] (Table 2)

Table 2 - APTES concentration on the MSN surface, calculated by ^1H NMR.

Sample	[APTES] (mmol/g)	[APTES] (APTES /nm^2)
MSN1+APTES	2.22	4.25
MSN2+APTES	1.66	2.07
MSN3+APTES	1.50	2.90
MSN4+APTES	2.12	4.10

This amino modification allows the immobilization of other molecules to the external surface of silica, which in this work is a RAFT agent. After this reaction the surfactant was removed by treating the particles with an ethanolic solution of chloridric acid (Step 4, Scheme 3).

3.2.2. Chain Transfer Agent (CTA) Modified MSNs

The RAFT agent used was 3-(benzylsulfanylthiocarbonylsulfanyl) propionic acid (BSPA). Its immobilization was achieved by reacting the carboxylic acid with the amine on the surface of the MSN (Step 5, Scheme 3). In order to quantify the amount of CTA molecules immobilized on the surface, UV-Vis spectroscopy was used. The RAFT agent exhibits an absorbance maximum around 310 nm. The UV-vis spectra of MSN+APTES (previous step) was used as a baseline to account for light scattering. [16]

The first results obtained showed that [CTA] = 5.99×10^{-3} mmol/g MSN (0.11 CTA molecule/nm^2). Since the CTA and the surface ligand were present in equimolar quantities it was expected that the RAFT agent's concentration was close to the one of APTES. This was attributed to two factors: the treatment used to remove the surfactant prior to the fixation of the CTA and stereochemical effects. On one hand, the acid treatment used to remove the template prompted the protonation of the amine groups reducing their nucleophilic character. Additionally, the attachment of each CTA molecule to the surface may have hindered subsequent reactions in its vicinity due to stereochemical hindrance. Since these effect forces a system change, in order to increase the quantity of CTA fixated on the surface, was on reverting the loss of nucleophilic character of the amine groups. This way, the particles were washed with an ethanolic solution of ammonia. The CTA concentration in the surface increase when compared to the first reaction, nonetheless, the concentration was significantly lower than the APTES concentration. However, the decision of not pursuing a higher CTA concentration was made because it was reported that termination reactions occur at a high rate at an early stage for surface densities as low as 0.08 chains of polymer/nm^2 (i.e. 0.08 CTA molecules/nm^2). [20]

After the preliminary results of the polymerization study (see section 3.4) it was decided to change the RAFT agent. Therefore, a new batch of nanoparticles was functionalized and the new CTA (4-Cyano-4-(phenylcarbonothioylthio)pentanoic acid (CPADB)) was immobilize by the same process as BSPA. (Table 3)

Table 3 - Concentration of CTA on the surface of the particles.

Sample	[CTA] (mmol/g)	[CTA] (CTA/nm^2)
MSN1+BSPA	1.35×10^{-1}	0.26
MSN2+BSPA	1.66×10^{-1}	0.21
MSN3+BSPA	3.34×10^{-2}	0.06
MSN4+CPADB	8.34×10^{-2}	0.16

3.3. ζ-Potential

Zeta potential was used as an additional parameter to assess the surface modification at each stage of this work. The measurements were made dispersing the samples in MilliQ water (pH = 5.5) (Table 4)

Table 4 - ζ-potential of MSN samples on every step of its surface modification measure.

Sample	ζ-Potential (mV)		
	MSN	MSN+APTES	MSN+CTA
MSN1	-28.0 ± 5.2	29.7 ± 5.2	8.1 ± 3.1
MSN2	-21.0 ± 3.3	30.0 ± 4.0	10.3 ± 3.1
MSN3	-13.0 ± 4.5	30.0 ± 4.8	30.2 ± 4.9
MSN4	-20.2 ± 3.3	28.0 ± 4.2	13.4 ± 3.8

It is possible to observe a significant change in each modification step. The bare MSNs without surfactant show a negative potential because the silanol groups have an (IEP) of 1.5, thus having a negative charge at pH higher than 1.5. The APTES-functionalized MSNs show positive potentials due to the presence of the amine function which shifts the Isoelectric Point to higher pH values, as the intrinsic pKa of the

aminopropyl is 9.8 and the IEP is 10.6, and the amino groups should be fully protonated at pHs less than about 9. [16] The immobilization of CTA in the MSN surface resulted in a substantial decrease of ζ-Potential, which indicates a successful surface modification. However, in the case of MSN3+CTA there was no ζ-Potential alteration. This can be explained by the low amount of CTA grafted onto the surface.

3.4. Polymerization Study

Prior to coating the MSNs with a polymer shell, it was necessary to confirm that the chosen RAFT agent (BSPA) was, indeed, controlling the polymerization. Furthermore, the reaction's kinetic should be determined to ascertain the optimal reaction conditions.

The polymerization was conducted in different conditions based on reports of RAFT polymerizations of DPA-containing copolymer. [21] From the results it was concluded that BSPA was not suitable for the polymerization of this monomer, because most of the molecules were being deactivated once the reaction started. It was decided to change the RAFT agent and a dithiobenzoate (CPADB) was chosen. New experiments were made to determine the optimal conditions for the reaction (see section 2.4, route 2). We obtained a polymer with a molecular weight of 12.8 kDa determined by GPC-MALS and UV-Vis spectroscopy. Since the targeted molecular weight was 10 kDa, this proved that CPADB was a suitable CTA to this monomer.

3.5. Nanoparticles with a pH-responsive shell

The approach idealized to modify the nanoparticle surface with a polymer was the "grafting from" method, in which, solely anchored RAFT agents would mediate the polymerization. However, non- published results of our group indicated a low incorporation of polymer using this method. Furthermore, it was reported that the addition of free RAFT agents in solution resulted in a increased polymer incorporation. This CTA excess in the polymerization mixture helps in exchanging oligomeric radicals between the grafted RAFT agents and in solution. [22]

With all this considered, the initial strategy was abandoned, and it was decided to use this approach, a hybrid grafting method (Step 6, Scheme 3). Aside from providing a higher polymeric grafting it also offers an opportunity of analysing the polymer grafted without destroying the particles, using the polymer that remains in the polymerization medium.

A polymer with M_n = 55 kDa was obtained, which is very close to the target (50 kDa). Furthermore, the $Đ$ = 1.04 confirms that the polymerization is being controlled. The polymerization incorporation obtained was 5.2 wt% (polymer/MSN), it is expected that the polymeric chains grafted on the surface are homogeneously dispersed and are enough to ensure a good coverage of the surface and reliable controlled delivery system.

The variation of hydrodynamic diameter (D_H) with pH for MSN4+PolyDPA was measured by DLS. For pH values lower than the pKa of the polymer shell, the polymer is in an expanded random coil conformation, with a D_H = 439 nm (diameter much larger than that of bare MSN, D_H = 182 nm). For pH values above the pKa the polymer shell collapses into a globule-like conformation and the size should be like the one of bare particles. However, it was not possible to measure this diameter, since with a collapsed shell the particles tend to aggregate.

3.6. Release Study

3.6.1. Incorporation of SRB

The aim of this proof of concept study was to test the controlled release of SRB incorporated in MSN4+PolyDPA. SRB was used due to its high quantum yield and water solubility. The control was achieved by modulating the pH.

There are two main strategies for drug loading, *in situ* during synthesis or as post-sorption (either by physisorption or by chemisorption). The latter is the most common approach to loading drugs into MSNs. The one used in this work was physical adsorption from solution into the mesopores, which is the most often used method for the loading of small molecules such as SRB. [24] In the present case, the presence of the positively-charged polymer shell not only ensure that the cargo was not prematurely released but also helped the adsorption of the negatively-charged SRB.

It was determined that the incorporation process yielded a concentration of 7.67×10^{-4} mol SRB/g MSN.

The release study consisted in changing the polymer shell as a response to a pH alteration. Since the polymer's pKa is about 6.5, we decided to modulate the pH of the dispersion of MSN4+PolyDPA (see section 2.2.7) between 5 and 9.

The emission ($\lambda_{excitation} = 566\,nm$) and excitation spectra ($\lambda_{emission} = 589\,nm$) of SRB

in PBS pH 5 and pH 9 (Figure 2) show the dependence of the SRB's quantum yield in pH.

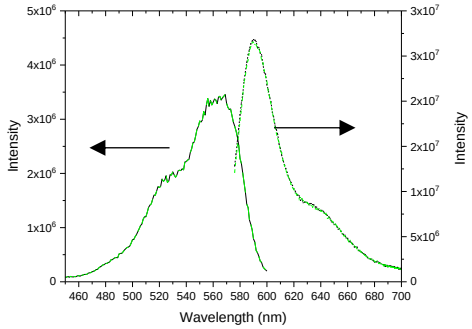

Figure 2 - Emission (dash, right) and excitation (lines, left) spectra of SRB at pH 5 (black) and pH 9 (green), with $\lambda_{excitation}$ = 566 nm and $\lambda_{emission}$ = 589 nm.

It is possible to observe that the SRB's quantum yield is independent from pH within the range used in this study.

3.6.2. Controlled Release

To monitor the release of SRB from the nanoparticles we used a fluorescence cuvette fitted with a top chamber separated from the bottom compartment by a dialysis membrane (see section 2.6, Scheme 2). It was important to determine the influence of pH in the dialysis device, specifically, how it impacted the diffusion across the membrane. A solution of SRB in PBS (pH 9) ($C = 4.37 \times 10^{-6}\ M$) was loaded into the dialysis device and the fluorescence intensity was monitored for 4 h, with additions of 10 µL [H_2SO_4] = 1M every hour. This changes the pH from 9 to 5 in the dialysis device, while the intervals between the additions ensure that the equilibrium is restored and the pH in the device is, again, close to 9.

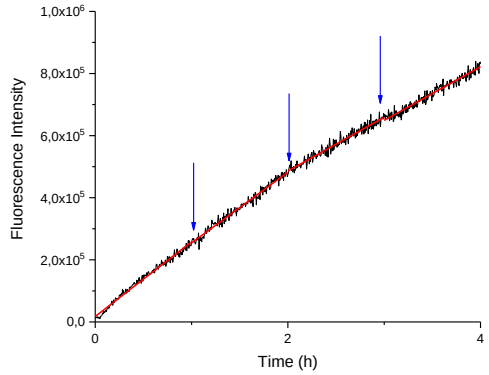

Figure 3 - Evolution of fluorescence intensity in compartment B due to the diffusion of free SRB from compartment A (black line), indication of acid additions (blue arrows) and linear fit of each section (red lines). $\lambda_{excitation}$ = 566 nm and $\lambda_{emission}$ = 589 nm.

From Figure 3 is possible to conclude that pH has no influence in the diffusion process across the cellulose membrane. To evaluate the degree of control over cargo release for the MSN4+PolyDPA we used the process described in section 2.6.

The degree of control over cargo release obtained for the nanoparticles was evaluated by continuously measuring the fluorescence of the cuvette, while modulating the pH between 5 and 9 in the dialysis device. The initial strategy was to make acid additions in the dialysis device, to low the pH from 9 to 5. These additions were to be sufficiently spaced to give time to the equilibrium (between the two compartments) to be restored, and the pH in the dialysis device return to a value close to 9.

It was expected to observe an increase in the fluorescence intensity at pH 5 (expanded polymeric chains, pores are open) and a stagnation once the equilibrium was restored and the pH value was closed to 9 (collapsed polymeric chains, closed pores).

The curve obtained through the monitorization of the fluorescence intensity in compartment B is presented in Figure 4, with indications of the acid (black arrows) and base (green arrows) additions. In red is presented a linear projection of the stagnation periods.

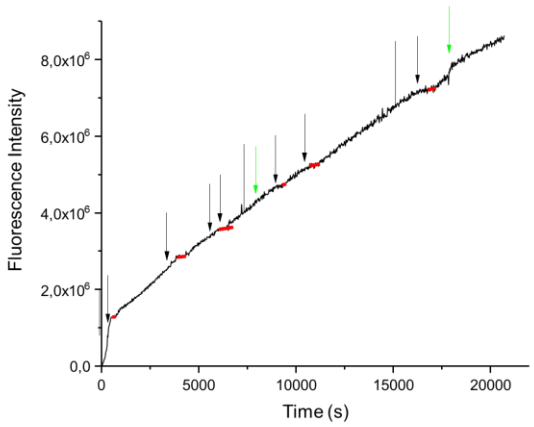

Figure 4 - Evolution of fluorescence intensity in compartment B and indications of acid additions (black arrows) and base additions (green arrows). $\lambda_{excitation}$ = 566 nm and $\lambda_{emission}$ = 589 nm.

During the experiment, it was observed that the system worked opposite to what was expected, i.e., the fluorescent intensity increased when the pH value surpasses the pKa of the polymer (pH>6.5) and, stagnated when acid was added (pH 5). This can be explained by the characteristics of the polymer shell and of the cargo used. After each acid addition the pH

decreases to 5 (pH below the polymer pKa) and the shell is protonated, and it expands allowing negatively-charged SRB molecules to diffuse from the mesopores to the surface. Due to the electrostatic interactions SRB molecules are trapped in the shell and are only released when the pH rises (above pKa) to reach equilibrium and the shell is deprotonated (collapsed). It is possible to observe a more pronounced release in the beginning due to the presence of SRB molecules adsorbed at the surface. The results obtained show that the hybrid system is able to control the release of its cargo by changing its polymer shell conformation as a response to pH changes.

The release curve was divided by sections, corresponding to the periods where the pH was lower (stagnation periods) and higher than the polymer's pKa. Since the volume in the bottom compartment of the dialysis device is constant, it was possible to obtain the rate of release. (Figure 5)

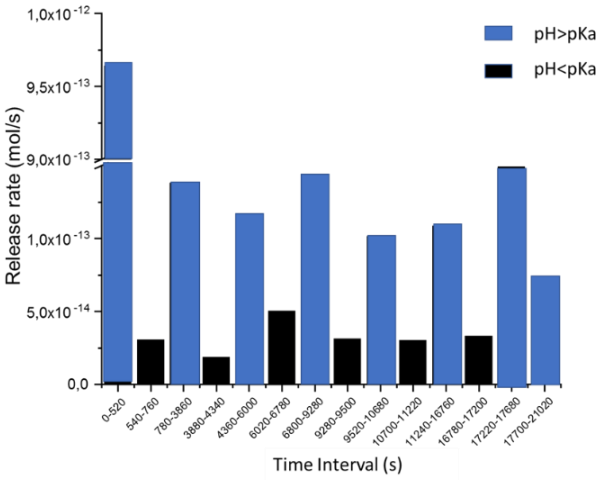

Figure 5 - Rate of SRB release of each section of the release, corresponding to the periods where the pH was lower (black collumns) and higher (black columns) than the polymer's pKa.

The data presented in Figure 5 confirm the conclusions drawn from the release curve. After each acid addition (pH 5 < pKa, black columns) the release rate abruptly drops. This corresponds to the stagnation periods observe in the release curve (Figure 4), when the SRB molecules diffuse from the mesopores and are trapped in the polymeric shell. The interval 6020-6780 s has a slightly higher rate, because accounts for a period where two consecutive additions of acid where made. However, when before the second addition was made, some SRB was already being released.

In conclusion, our system is able to control the release of its cargo by changing its polymer shell conformation as a response to pH changes. It presents a low release rate at acidic pH values and a large release rate at basic pH values. This behaviour is not suitable for cancer treatment, since tumour tissues have a more acidic extracellular environment than the corresponding healthy tissues. However, this behaviour can change depending on the cargo's electrostatic nature. It is expected to observe an opposite behaviour for a cargo with no charge, since there will not be interaction with the polymer shell. Therefore, we are confident that our system has the potential to be used as a carrier of anti-cancer drugs.

4. Conclusion

In this work a novel carrier for controlled release, based on mesoporous silica nanoparticles coated with a pH-responsive polymer shell, was prepared. TEM and DLS confirmed the success on the synthesis of spherical MSN with narrow size dispersity. Different NaOH concentrations yielded nanoparticles of different sizes due to the electrostatic interaction between OH^- groups (after TEOS hydrolysis) and the positive charges at the micelles surface. The charge screening induces the micelle aggregation, increasing the supramolecular aggregation number, and producing larger nanoparticles.

The particles were submitted to amine surface modification process using APTES. These molecules allow to immobilize CTA molecules for the controlled polymerization of DPA from the surface.

The polymer shell-coated MSN were obtained using a hybrid "grafting from" approach, to increase the polymer incorporation in the particles surface, in comparison with a pure "grafting from" approach. The polymer incorporation was determined to be 5 wt% polymer/particle by ^1H NMR. Furthermore, using this hybrid "grafting from" approach it was possible to characterize the incorporated polymer by analysing the chains present in the supernatants. The characterization was made by UV-Vis spectroscopy and GPC-MALS.

In the proof-of-concept release experiments, we use a model molecule (SRB) modulating the pH between 5 and 9. The results show a strong influence of the polymer shell coating on the release kinetics, with the system behaviour being similar to a sponge: the cargo diffuses into the polymer shell at pH values around 5 and is released when the pH rises above pKa (≈6.5)

when the shell collapses, producing a pumping action that releases the cargo.

5. References

[1] Bharti, Charu and Neha Gulati. 2015. “Mesoporous Silica Nanoparticles in Target Drug Delivery System: A Review.” *International Journal of Pharmaceutical Investigation* 5(3):124.

[2] Desai, Manisha P., and Vinod Labhasetwar. 1997. “The Mechanism of Uptake of Biodegradable Microparticles in Caco-2 Cells Is Size Dependent.” *Pharmaceutical Research* 14(11):1568–73.

[3] Zauner, W., N. A. Farrow, and A. M. Haines. 2001. “In Vitro Uptake of Polystyrene Microspheres: Effect of Particle Size, Cell Line and Cell Density.” *J Control Release* 71(1):39–51.

[4] Mohanraj, V. J. and Y. Chen. 2006. “Nanoparticles – A Review.” *Tropical Journal of Pharmaceutical Research* 5:561–73.

[5] Argyo, Christian and Veronika Weiss. 2013. “Multifunctional Mesoporous Silica Nanoparticles as a Universal Platform for Drug Delivery.” *Chemistry of Materials* (26):435–51.

[6] Schulz, Anja and Colette Mcdonagh. 2012. “Intracellular Sensing and Cell Diagnostics Using Fluorescent Silica Nanoparticles.” *Soft Matter* (8):2579–85.

[7] Stober, W. 1968. “Controlled Growth of Monodisperse Silica Spheres in the Micron Size Range 1.” *Journal of Colloid and Interface Science* 69:62–69.

[9] Si-Han Wu and Chung-Yuan Moua. 2013. “Synthesis of Mesoporous Silica Nanoparticles.” *Chemical Society Reviews* 42(9):3862.

[10] Kresge, C. T. and M. E. Leonowicz. 1992. “Ordered Mesoporous Molecular Sieves Synthesized by a Liquid-Crystal Template Mechanism.” *Nature*, 359.

[11] Grün, Michael and Iris Lauer. 1997. “The Synthesis of Micrometer- and Submicrometer-Size Spheres of Ordered Mesoporous Oxide MCM-41.” *Advanced Materials* 9(3):254–57.

[12] Cayre, Olivier J. and Simon Biggs. 2011. “Stimulus Responsive Core-Shell Nanoparticles : Synthesis and Applications of Polymer Based Aqueous Systems.” *Soft Matter* (7):2211–34.

[13] Baleizão, Carlos and J. P. S. Farinha. 2015. “Hybrid Smart Mesoporous Silica Nanoparticles for Theranostics.” *Nanomedicine* 10:2311–14.

[14] Chaudhuri, Rajib Ghosh. 2012. “Core / Shell Nanoparticles : Classes , Properties , Synthesis Mechanisms , Characterization , and Applications.” *Chemical Society Reviews* (112):2373–2433.

[15] Favier, Arnaud and Marie Thérèse Charreyre. 2006. “Experimental Requirements for an Efficient Control of Free-Radical Polymerizations via the Reversible Addition-Fragmentation Chain Transfer (RAFT) Process.” *Macromolecular Rapid Communications* 27(9):653–92.

[15] Gao, Weiwei and Juliana M. Chan. 2010. “PH-Responsive Nanoparticles for Drug Delivery.” *Molecular Pharmaceutics* 7(6):1913–20.

[16] Santiago, Ana M., Carlos Baleizão, and J. P. S. Farinha. 2015. “Multifunctional Hybrid Silica Nanoparticles with a Fluorescent Core and Active Targeting Shell for Fluorescence Imaging Biodiagnostic Applications.” *European Journal of Inorganic Chemistry* (27):4579–87.

[17] Ribeiro, T., C. Baleizão, and J. P. S. Farinha. 2017. “Hybrid Mesoporous Silica Nanocarriers with Thermovalve-Regulated Controlled Release.” *Nanoscale* 13485–94.

[18] Chiang, Ya-dong and Hong-yuan Lian 2011. “Controlling Particle Size and Structural Properties of Mesoporous Silica Nanoparticles Using the Taguchi Method.” *The Journal of Physical Chemistry* (115):13158–65.

[19] Crucho, Carina I. C., Carlos Baleizão, and José Paulo S. Farinha. 2017. “Functional Group Coverage and Conversion Quantification in Nanostructured Silica by 1 H NMR.” *Analytical Chemistry* 89(1):681–87.

[20] Tsujii, Yoshinobu and Muhammad Ejaz “Mechanism and Kinetics of RAFT-Mediated Graft Polymerization of Styrene on a Solid Surface.” *Macromolecules* 8872–78.

[21] Hu, Ying Qian and Min Sang Kim.2007. “Synthesis and PH-Dependent Micellization of 2-(Diisopropylamino)Ethyl Methacrylate Based Amphiphilic Diblock Copolymers via RAFT Polymerization.” *Polymer* 48(12):3437–43.

[22] Kutcherlapati, S. N. Raj. and Rambabu Koyilapu. 2017. “Glycopolymer-Grafted Nanoparticles: Synthesis Using RAFT Polymerization and Binding Study with Lectin.” *Macromolecules* 50(18):7309–20.